Journal of Materials Chemistry C

Design of *p*-type Transparent Conducting Oxide Sn_2GeO_4 by ab initio Evolutionary Structure Search

Journal:	*Journal of Materials Chemistry C*
Manuscript ID	TC-ART-08-2018-004024.R1
Article Type:	Paper
Date Submitted by the Author:	27-Sep-2018

Complete List of Authors:	YU, JUN; National Institute of Advanced Industrial Science and Technology Tsukuba Center Tsukuba Central Wang, Junjie; Tokyo Institute of Technology, Materials Research Center for Element Strategy Kumar, Mukesh; National Institute for Materials Science, Environmental Remediation Materials Unit; Thapar University, School of Physics and Materials Science Umezawa, Naoto; National Institute for Materials Science (NIMS), International Center for Materials Nanoarchitectonics (MANA) Abe, Hideki; National Institute for Materials Science,

Journal of Materials Chemistry C

ARTICLE

Design of *p*-type Transparent Conducting Oxide Sn_2GeO_4 by ab initio Evolutionary Structure Search

Jun Yu[#, a], Junjie Wang[#, *, b, c, d], Mukesh Kumar[b, e], Naoto Umezawa[*, b, f], Hideki Abe [*, d]

Received 00th January 20xx,
Accepted 00th January 20xx

DOI: 10.1039/x0xx00000x

www.rsc.org/

In contrast to *n*-type transparent conducting oxides, very few *p*-type transparent conducting oxides have been discovered till date. In this work, we predicted two new tin-germanates based compounds (Sn_2GeO_4) as potential *p*-type transparent conducting oxides having exceptionally low hole effective masses and wide band gap energies. Through detailed electronic structure calculations, we revealed that Sn_2GeO_4 compounds possess sufficiently wide band gap (3.24 eV) for transparency and very small effectie mass (0.46) for hole carrier due to the influence of divalent Ge^{2+}. Our study show the potential of band engineering of Sn^{2+} and Ge^{2+} cations with (n-1)d^{10}ns^2 electronic configuration as *p*-type TCOs, which can expand the materials family for the future design and development of *p*-type transparent conducting oxides.

Introduction

Transparent conducting oxides (TCOs) can be classified into two groups, i.e. *n*-type and *p*-type, based on their mobile charge carriers are electrons or holes. While *p*-type TCOs have drawn more attention since the discovery of promising p-type conductivity of $CuAlO_2$,[1] they are still much rarer than their *n*-type counterparts. Recently, tin monoxide (SnO) has been proven to have the potential as a *p*-type semiconductor.[2] However, the narrow band gap (0.70 eV) of SnO prevents it to be the perfect transparency required for TCOs. The feasible way to extend the band gap is to mix the divalent tin in SnO and tetravalent tin in SnO_2 together to synthesize new tin oxides. Some structures of mixed-valence tin oxides, which include Sn_3O_4 and Sn_2O_3, have been reported experimentally and theoretically. [3-10] Recently, we have conducted an extensive theoretical study of crystal structure search and electronic structure calculation of mixed-valence Sn_xO_y compounds.[11] A series of stable structures of mixed valence tin oxides, e.g. Sn_2O_3, α-Sn_3O_4, β-Sn_3O_4 and Sn_5O_6, have been confirmed. α-Sn_3O_4 and β-Sn_3O_4 show a perspective as *p*-type TCOs with band gaps of 2.78 eV and 3.25 eV, respectively. However, our preliminary research shows that their valence band tops are too flat to produce small effective mass of hole, which is necessary for *p*-type TCOs application. To obtain *p*-type TCOs, Kawazoe et al.[12] once proposed a possible scheme to form an extended valence band structure through introducing the covalence in the metal-oxygen bonding. Germanium (Ge) is a good choice of cationic species for the enhancement of covalence with oxygen since energy level of divalent Ge is close to that of oxygen *p* states similar to the case of Sn^{2+} in Sn_3O_4. The closed shell *d* electronic configuration of Ge is also advantageous for preventing coloration. Mizoguchi et al.[13] have synthesized cubic $SrGeO_3$, a new Ge-based TCO and expands the family of TCOs from ionic oxides to covalent oxides. This discovery also encourages us to search possible Sn-Ge-O compounds for TCOs application because this system can possess both of divalent tin and germanium, which are promising elements to enhance hybridization with oxygen *p* states. Recently, computational materials informatics including high-throughput screening[14-16] and evolutionary structure search[11], has become an alternative method to experiment in designing new p-type TCOs. Based on the previous study of Sn^{2+}-based TCOs,[11, 16] we carried out a detailed Sn-Ge-O compounds search by employing the evolutionary algorithm.[17-19] Two stable Sn-Ge-O compounds possessing low hole effective mass and wide band gap were confirmed and proposed as *p*-type TCO candidates. In addition to the identification of Sn-Ge-O compound structures, the underlying reasons for those exceptionally low hole effective masses were studied using electronic structure calculations. To the best of our knowledge, this is the first dedicated study to search the possible Sn-Ge-O TCOs by theoretical method.

[a.] *Advanced Manufacturing Research Institute, National Institute of Advanced Industrial Science and Technology, 1-2-1 Namiki, Tsukuba, Ibaraki, Japan.*
[b.] *International Center for Materials Nanoarchitectonics (MANA), National Institute for Materials Science, 1-1 Namiki, Tsukuba, Ibaraki 305-0044, Japan.*
[c.] *Materials Research Center for Element Strategy, Tokyo Institute of Technology, 4259 Nagatsuta-cho, Midori-ku, Yokohama, Kanagawa 226-8503, Japan*
[d.] *Center for Green Research on Energy and Environmental Materials, National Institute for Materials Sciences, Ibaraki 305-0044, Japan.*
[e.] *School of Physics and Materials Sciences, Thapar University, Patiala, Punjab 147004, India*
[f.] *Samsung Electronics, Semiconductor R&D Center, 1, Samsungjeonja-ro, Hwaseong-si, Gyeonggi-do 18448, Korea*
[#] *These authors contributed equally.*
[*] *Email - wang.junjie0810@gmail.com; umezawa.naoto@gmail.com; abe.hideki@nims.go.jp*
Electronic Supplementary Information (ESI) available. See:
DOI: 10.1039/x0xx00000x

Computational Methods

In this work, we carried out an extensive structure searching of Sn-Ge-O compounds and electronic structure calculations for obtained stable structures through combining first principles calculation and an evolutionary structure search algorithm USPEX (Universal Structure Prediction: Evolutionary Xtallography).[17-19] In the structure search process, the global optimization, which produced new structure through variation operations based on the evolutionary algorithm (such as heredity, permutation, mutation, soft mutation...), and the local optimization, which optimized the generated structures, were respectively done using USPEX and VASP (Vienna ab initio simulation package)[20] codes. The first-principles calculations were carried out using the generalized gradient approximation (GGA) in the Perdew–Burke–Ernzerhof (PBE)[21] form as implemented in VASP. Relatively rough calculation settings were used in the structure searching to save the time for optimizing thousands of structure. Energy cutoff of 400 eV and spacing of around $2\pi \times 0.05$ Å^{-1} were set for the plane-wave basis set and the Monkhorst–Pack k-point mesh. The optimized structures of α-Sn_3O_4 and β-Sn_3O_4 in the previous study[11] were used as prototypes in our structure searching of Sn-Ge-O compounds. The most stable structures obtained in the structure search were re-optimized using energy cutoff of 600 eV and k-mesh resolution of $2\pi \times 0.02$ Å^{-1}. The electronic structures, optical absorption and defect formation energy calculations of predicted structures were performed by employing the screened non-local exchange-correlation density functional (HSE06).[22] We computed the band structures by HSE06 with a rigid shift of the conduction band (scissor operator) to fit the band gap to the GW ('G' is the Green's function, 'W' represents the screened Coulomb interaction) value.[23] Among various GW approximations, we used partially self-consistent GW (scGW0) approach using PBE wavefunction, where the Green's function 'G' is updated iteratively, whereas the screened Coulomb potential 'W' was kept fixed.

Results and Discussion

Through sampling over 5000 structures with different Sn-Ge-O compositions, two structures (Fig.1) with the formula of Sn_2GeO_4 were obtained, which possess the space groups P-1 and P21/c, respectively. The crystal information of these two predicted structures together with the structure data of previously reported Sn_3O_4[11] can be referred in the Table S1 of the Supporting Information. Similar with Sn_3O_4, the two Sn_2GeO_4 crystals are layered structures. The dynamic stabilities of these two new structures were both confirmed by the phonon dispersion calculations shown in Fig. 1. However, the calculated reaction energies reveal that only α-Sn_2GeO_4 is thermodynamically stable with respected to known compounds SnO and GeO_2 with a negative reaction energy of -0.008 eV/atom. The β-Sn_2GeO_4 could be a metastable phase with a slightly positive reaction energy of 0.003 eV/atom (Supporting Information Table S2). Comparing with α-Sn_3O_4 and β-Sn_3O_4, Bader charge analysis (Table S3 in Supporting Information) shows that the total charges of cations in α-Sn_2GeO_4 and β-Sn_2GeO_4 are respectively decreased from 9.907 |e| in α-Sn_3O_4 to 9.809 |e| and from 9.932 |e| in β-Sn_3O_4 to 9.709 |e|, which indicates the increase of the covalence of Sn_2GeO_4 compounds compared with that of Sn_3O_4. Therefore, we can expect that the dispersion of the valence bands of Sn_2GeO_4 would be enhanced according to the scheme proposed by Kawazoe et al.[12]

The calculated band structure (Fig. 2 (a)) shows that the band gap (3.24 eV) of α-Sn_2GeO_4 is significantly increased compared with that of α-Sn_3O_4 (2.78 eV as shown in Supporting Information Fig. S1(a)).[11] On the other hand, band gap of β-Sn_2GeO_4 (3.20 eV), as shown in Figure 2 (b), is almost identical with β-Sn_3O_4 (3.25 eV as shown in Supporting Information Fig. S1(b)). Our previous study[12] revealed that the band gap of α-Sn_3O_4 and β-Sn_3O_4 are determined by the states of divalent tin. Similarly, the projected density of states (DOS) for α-Sn_2GeO_4 and β-Sn_2GeO_4 (shown in Figs. 2 (c) and (d) in comparison with those of α-Sn_3O_4 and β-Sn_3O_4) reveal that the valence band maximum (VBM) and conduction band minimum (CBM) of these two structures are both determined by the states of divalent cations: Ge^{2+} and Sn^{2+}. To form α-Sn_2GeO_4, two of four divalent tin atoms in the lattice of α-Sn_3O_4 (Table S1 in Supporting Information) are replaced by divalent germanium atoms. This results in opening the band gap of α-Sn_2GeO_4 compared with that of α-Sn_3O_4 due to the strong covalent nature of Ge-O bonds (Fig. 2(c)) and weakened inter-layer cation interactions as discussed below. The germanium atoms in β-Sn_2GeO_4 locate at the center of each layer and possess tetravalence. Hence the band gap of β-Sn_2GeO_4 is almost same with that of β-Sn_3O_4 (Supporting Information Fig. S1(b)) because both of their VBM and CBM are determined by the states of interlayer Sn^{2+}. However, the Sn^{2+} (5*s*) states in β-Sn_2GeO_4 gets spread wider than those in β-Sn_3O_4 (Fig. 2(d)) in the valence band region near VBM.[11] The influence of Ge^{2+} on the band gaps of Sn_2GeO_4 compounds will be discussed in detail in the latter part using crystal orbital overlap populations (COOPs) analysis.

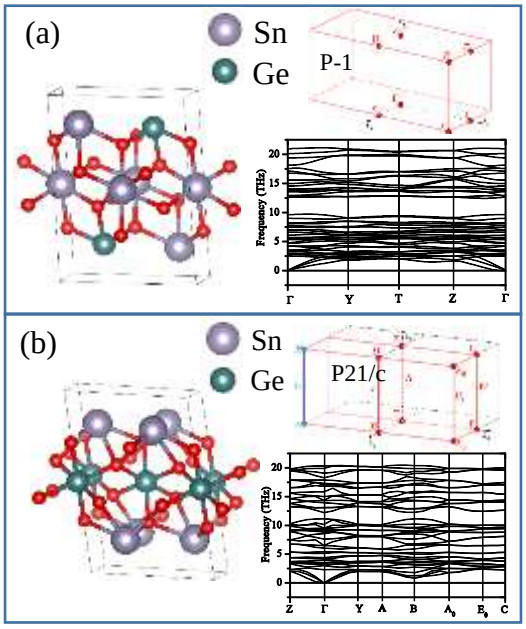

Figure 1 Crystal structures, Brillouin zones and phonon dispersions of predicted (a) α-Sn_2GeO_4 and (b) β-Sn_2GeO_4.

The partial charge densities at the VBM and CBM (Figs. 2 (e) and (f)) show that both the VBM and CBM mainly consist of cation states located at interlayer surfaces, i.e. Sn^{2+} and Ge^{2+} derived states for α-Sn_2GeO_4 and Sn^{2+}-derived state for β-Sn_2GeO_4, which is consistent with the projected density of states (DOS) (Fig. 2 (c) and (d)). Furthermore, the strong dispersions of the band structures at the VBM for both α-Sn_2GeO_4 and β-Sn_2GeO_4 (Figs. 2 (a) and (b)) are beneficial to produce small mass of hole, which is confirmed by the calculation of effective masses of the hole (m_h^*) in the unit of free-electron mass for α-Sn_2GeO_4 and β-Sn_2GeO_4 along each direction in the reciprocal space (Supporting Information Table S4). The calculated effective masses of hole along [100] (α-phase: 0.53; β-phase: 0.032), [010] (α-phase: 0.11; β-phase: 0.060) and [001] (α-phase: 0.80; β-phase: 0.063) of two Sn_2GeO_4 compounds are exceptionally lighter than those of α-Sn_3O_4 (2.01, 0.28 and 0.24). This is especially truth in β-Sn_2GeO_4 and is a great advantage for *p*-type TCOS applications.

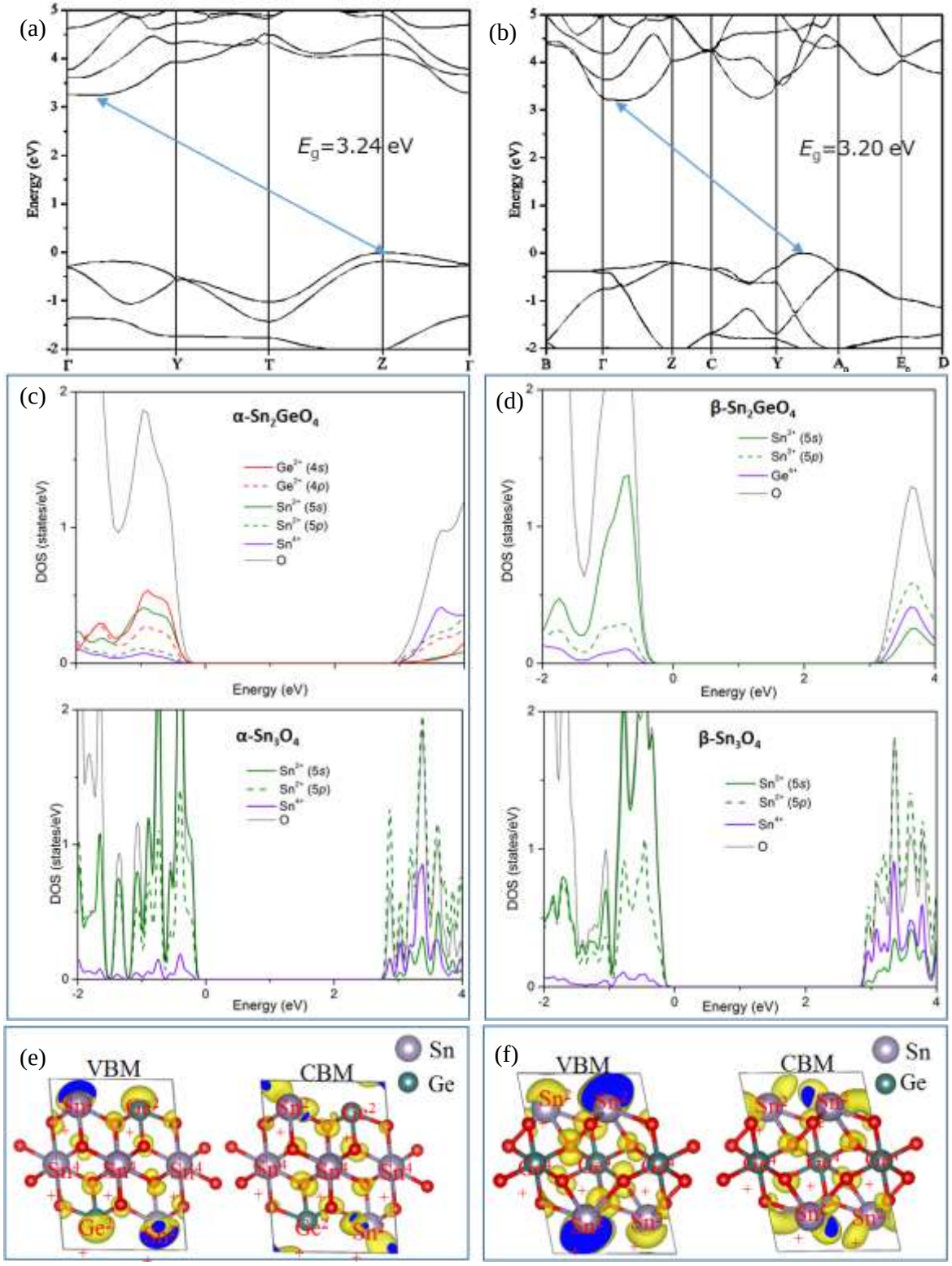

Figure 2 Band structures ((a) and (b)), projected density of states (in comparison with those of α- and β-Sn_3O_4) ((c) and (d)) and partial charge densities ((e) and (f)) at valence band maximum (VBM) and conduction band minimum (CBM) for predicted α-Sn_2GeO_4 ((a), (c) and (e)) and β-Sn_2GeO_4 ((b), (d) and (f)). The positions of VBM and CBM are indicated by arrows in (c) and (d).

An important criterion for assessing the capability of Sn_2GeO_4 compounds as p-type TCO materials is the photoabsorption coefficient. Figure 3 (a) shows the calculated photoabsorption coefficients for α-Sn_2GeO_4 and β-Sn_2GeO_4 in comparison with those of SnO_2 and α-Sn_3O_4, a well-known n-type TCO and a bi-polar semiconductor. Both of the α-Sn_2GeO_4 and β-Sn_2GeO_4

exhibit zero absorption in virtually entire range of visible light (1.65-3.26 eV). It shows that the transparency of Sn_2GeO_4 should be much improved as compared with α-Sn_3O_4 and is comparable with that of SnO_2. Therefore, the zero absorption and suitable band gaps for a broad range of wavelengths in the solar spectrum suggest that Sn_2GeO_4 in discovered structures have great potential for application in p-type TCOs.

To further confirm the potential of α-Sn_2GeO_4 as p-type TCO, we performed DFT calculations for charged defects using a supercell model. Although both of the α-Sn_2GeO_4 and β-Sn_2GeO_4 show promise as p-type TCOs, we only conducted defects calculations for the most stable alpha phase (Supporting Information Figure S2). The formation energy of defect D_X with charged states q in α-Sn_2GeO_4 is given by

$$E_f(D_X^q) = E_{tot}(D_X^q) - E_{tot}(\alpha\text{-}Sn_2GeO_4) - \sum_X n_X \mu_{D_X} + qE_F \quad (1)$$

Where $E_{tot}(D_X^q)$ and $E_{tot}(\alpha\text{-}Sn_2GeO_4)$ are respectively the total energies of the supercell with a defect D_X in charge state q and that of a perfect supercell without defect. n_X is the number of element X (Sn, Ge, O and H) that has been introduced ($n_X > 0$) or removed ($n_X < 0$) from the perfect supercell. μ_{D_X} is the chemical potential of element X and depends on the experimental growth or annealing conditions. The chemical potentials $\tilde{\mu}_{DX}$ can be referenced to the calculated energies of elemental phases: $\tilde{\mu}_{\mathrm{metal}} = \mu_{\mathrm{metal}} - E_{tot}[\mathrm{metal_{bulk}}]$; $\tilde{\mu}_O = \mu_O - 0.5E_{tot}[O_2]$; $\tilde{\mu}_H = \mu_H - 0.5E_{tot}[H_2]$ To synthesize α-Sn_2GeO_4, the chemical potentials of constituent elements, which are referenced to the energies of the elemental phases, need to satisfy

$$2\tilde{\mu}_{Sn} + \tilde{\mu}_{Ge} + 4\tilde{\mu}_O = \tilde{\mu}_{Sn2GeO4} \quad (2)$$

where $\tilde{\mu}_{Sn2GeO4}$ corresponds to the enthaly of formation of Sn_2GeO_4: $\Delta H_f(Sn_2GeO_4)$=-12.9 eV. To avoid the precipitation of unwanted compounds, e.g. SnO_2, GeO_2 and SnO, following conditions and Eq. (2) should be satisfied simultaneously: $\tilde{\mu}_{SnO2} > \tilde{\mu}_{Sn} + 2\tilde{\mu}_O$; $\tilde{\mu}_{GeO2} > \tilde{\mu}_{Ge} + 2\tilde{\mu}_O$; $\tilde{\mu}_{SnO} > \tilde{\mu}_{Sn} + \tilde{\mu}_O$.
In addition, the referenced chemical potential of each element must be negative: $\tilde{\mu}_{Sn} < 0$, $\tilde{\mu}_{Ge} < 0$ and $\tilde{\mu}_O < 0$ ($\tilde{\mu}_{Ge} > -2\tilde{\mu}_{Sn} + \tilde{\mu}_{Sn2GeO4}$). Consequently, Figure 3(b) shows that α-Sn_2GeO_4 can only be synthesized in the metal-rich region shadowed by the red lines.

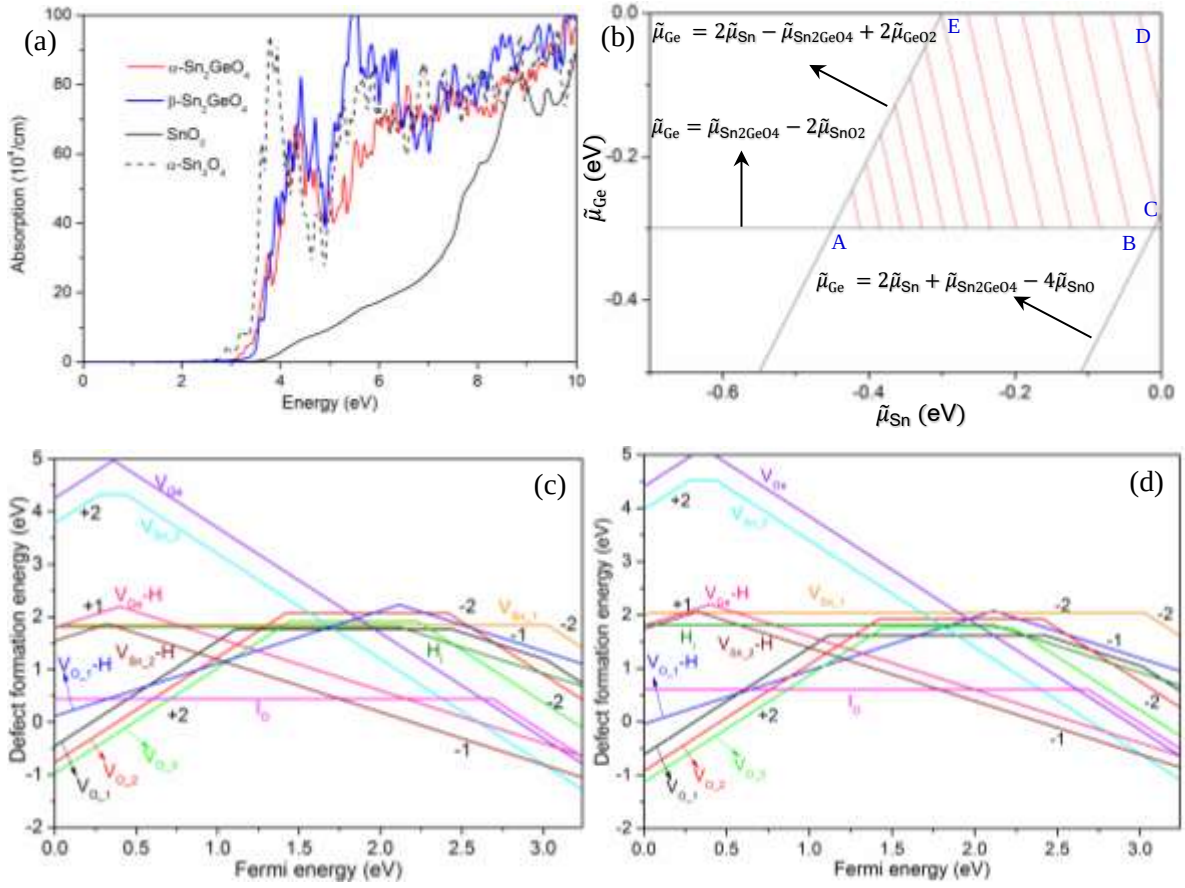

Figure 3 (a) Calculated optical absorption coefficients of α-Sn_2GeO_4 and β-Sn_2GeO_4 plotted in comparison with those of SnO_2 and α-Sn_3O_4 , chemical potential diagram associated equilibrium growth of α-Sn_2GeO_4 and formation energies of native point defects in α-Sn_2GeO_4 for (c) O-rich and (d) O-poor conditions.

Seven native point defects, i.e., oxygen interstitials IO, oxygen vacancies V_{O_1}, V_{O_2} and V_{O_3}, germanium vacancy V_{Ge}, and tin vacancies V_{Sn_1} (tetravalent Sn) and V_{Sn_2} (divalent Sn), were considered in the present study. For extrinsic defects, we

only considered H impurities since it is normally present in all growth environments of semiconductors. As pointed out by Van de Walle and co-workers, hydrogen can bind strongly with tin vacany in SnO to form V_{Sn}-H complex, which can act as a shallow acceptor to promote p-type conduction.[24] Therefore, three complexes formed through the interaction of H atoms with divalent Sn and Ge vacancies and oxygen vacancy in α-Sn_2GeO_4, i.e. V_{Sn_2}-H, V_{Ge}-H and V_{O_1}-H, were studied together with a hydrogen interstitial defect H_i in present work (shown in Figure S2). Figure 3 (c) and (d) shows the formation energies of these defects as a function of the Fermi energy under oxygen-rich (point A in Fig. 3(b)) and oxygen-poor (point E in Fig. 3(b)) conditions, respectively. Unlike *n*-type TCOs such as SnO_2, the oxygen vacancy can act as both donor and acceptor, although their thermodynamic transition levels are very deep, with (+2|0) transition levels at 1.1~ 1.4 eV above the VBM and (0|-2) transition levels at 0.2~0.9 eV below the CBM. Similarly, I_O is a deep acceptor having a thermodynamic (0|-2) transition level at 0.5 eV below the CBM. Therefore, these native defects are not able to generate a significant amount of carrier. However, it shows that the V_{Sn_2}-H and V_{Ge}-H complexes are relatively stable in various charge states. The formation energies of V_{Sn_2}-H and V_{Ge}-H are respectively much lower than those of isolated V_{Sn_2} and V_{Ge}. The V_{Sn_2}-H and V_{Ge}-H complexes are both shallow acceptors with (+/-) transition levels at 0.32 and 0.40 eV above the VBM, respectively. Moreover, the formation energies of V_{O_1}-H and interstitial H_i are higher than those of V_{Sn_2}-H and V_{Ge}-H under O-rich condition. The stability of negative charged V_{O_1}-H only gets enhanced on the metal-rich limit (Fig. 3 (d)). However, due to the presence of V_{Sn_2}-H, the Fermi levels under O-rich and O-poor conditions, which can be determined by the intersection of the lines of the most stable negative and positive charged defects, are respectively shifted downwards from 1.50 eV (intersection of V_{O_3} and V_{Sn_2}) to 1.10 eV (intersection of V_{O_1}-H and V_{Sn_2}-H) and from 1.75 eV (intersection of V_{O_3} and V_{Sn_2}) to 1.15 eV (intersection of V_{O_1}-H and V_{Sn_2}-H). It shows that defect V_{Sn_2}-H plays important role in suppressing the hole-killing effect of oxygen vacancies, holding the intrinsic Fermi level being situated below the middle of the band gap of α-Sn_2GeO_4. This indicates that the presence of H defects is very helpful in realizing p-type conductivity in α-Sn_2GeO_4.

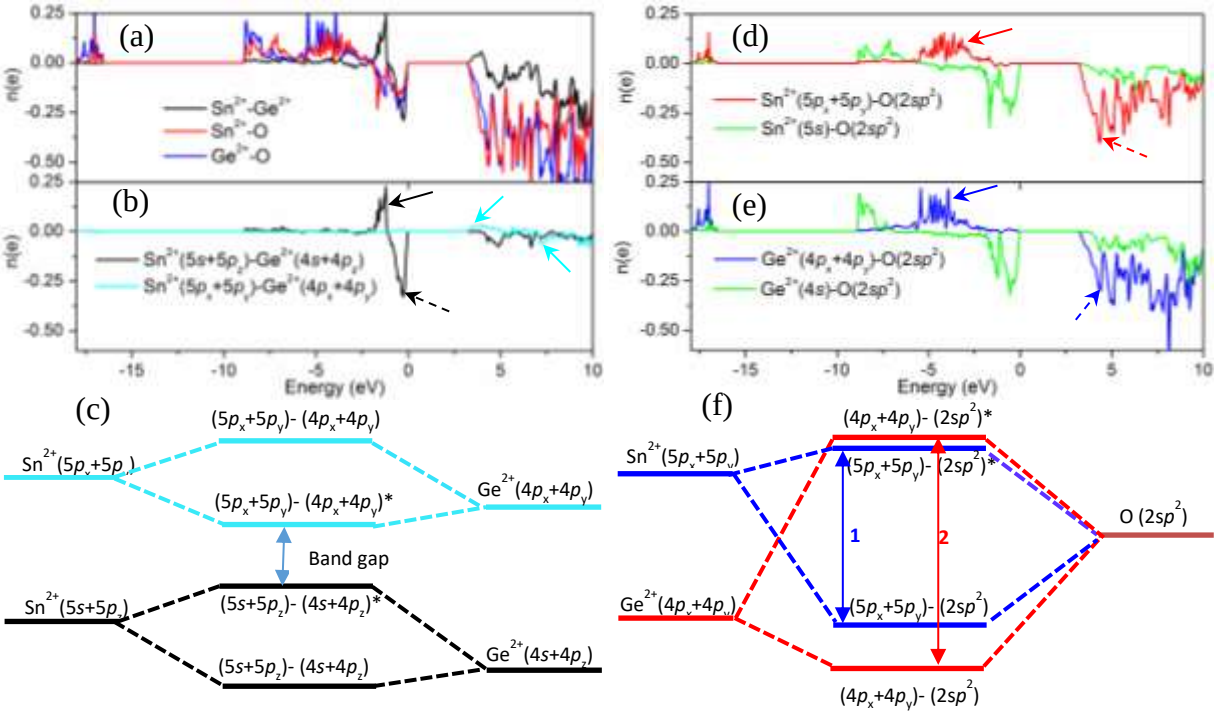

Figure 4 Crystal orbital overlap populations and energy level diagrams for α-Sn_2GeO_4. (a) Sn^{2+}-Ge^{2+}, Sn^{2+}-O and Ge^{2+}-O interactions; (b) Decomposed Sn^{2+}-Ge^{2+} interactions; (c) Energy level diagram for Sn^{2+}-Ge^{2+} interaction; (d) Decomposed Sn^{2+}-O interactions; (d) Decomposed Ge^{2+}-O interactions; (f) Energy level diagram for Sn^{2+}-O and Ge^{2+}-O interactions. The peaks corresponding to bonding and anti-bonding states in (c) and (f) are labelled by solid (bonding) and dashed (anti-bonding) arrows in (b), (d) and (e).

The crystal orbital overlap populations (COOPs), which are density-of-states-weighted overlap populations between two orbital centers, were calculated and shown in Fig. 4 for α-Sn_2GeO_4 to gain further insight into the evolution of the band structure. The positive and negative regions of COOP represent bonding and antibonding interactions between corresponding atomic orbitals, respectively. The calculated DOS (Fig. 2 (c) and (d)) shows that the contribution from O, Sn^{2+} and Ge^{2+} is dominant over other interactions at the VBM and CBM of Sn_2GeO_4. This means interactions between the divalent Sn^{2+} and

Ge2+ (interlayer) and the Sn^{2+}-O and Ge^{2+}-O (intralayer) interactions determines the band gaps of Sn_2GeO_4. To simplify the discussion, the present COOP calculations (Figs. 4 (a), (b), (d) and (e)) only show the interlayer Sn^{2+}- Ge^{2+} interactions and intra-layer Sn^{2+}-O and Ge^{2+}-O interactions around the Fermi level. Two energy level diagrams were constructed and shown in Figs. 4 (c) and (f) based on the COOP calculation results to well explain the mechanism of band gap widening of α-Sn_2GeO_4 in comparison with that of α-Sn_3O_4 (Fig. S1 (a)). The energy diagram in Fig 4 (c) shows that the anti-bonding state of $Sn^{2+}(5s+5p_z)$–$Ge^{2+}(4s+4p_z)$ interaction consists of the VBM and the bonding states of $Sn^{2+}(5p_x+5p_y)$–$Ge^{2+}(4p_x+4p_y)$ interaction contributes to the formation of CBM. Meanwhile, Figure 4 (f) reveals that the CBM is dominantly composed of $Sn^{2+}(5p_x+5p_y)$-O($2sp^2$) antibonding for the Sn-O interaction and $Ge^{2+}(4p_x+4p_y)$-O($2sp^2$) antibonding for the Ge-O interaction.

Moreover, the Bader charge calculations (Table S3 in Supporting Information) revealed that the covalence of Ge-O bonding in α-Sn_2GeO_4 is enhanced in comparison with that of Sn-O bonding in α-Sn_3O_4. Therefore, we can expect the interaction of $Ge^{2+}(4p_x+4p_y)$-O($2sp^2$) is stronger than the $Sn^{2+}(5p_x+5p_y)$-O($2sp^2$) in α-Sn_3O_4. Indeed, Figure 4 (f) shows that the distances between the bonding and antibonding states of Ge-O interactions are enlarged than those of Sn-O interactions (Figs. 4 (d), (e) and (f)), which lead to the upshift of CBM and the widening of the band gap of α-Sn_2GeO_4 compared to that of α-Sn_3O_4. This trend is the same as the band gap comparison between SnO_2 and GeO_2.[25, 26] Although Fig. 4 (e) shows that the $Ge^{2+}(4s)$-O($2sp^2$) interaction has contribution on the VBM, the influence of Sn^{2+}–Ge^{2+} interaction is dominant for the determination of VMB as shows in Fig. 4 (a).

Conclusions

In summary, we have performed a comprehensive structure search for the Sn-Ge-O system and identified two stable structures of α-Sn_2GeO_4 and β-Sn_2GeO_4 through employing first-principles evolutionary structure search algorithm. Both predicted compounds show layered structures and possess wide band gaps, low hole effective masses and zero photoabsorption coefficients in the most range of visible light, therefore, are promising for *p*-type TCO application. Furthermore, our defects study demonstrates that α-Sn_2GeO_4 is a promising *p*-type semiconductor because shallow-acceptor defects can be obtained through the formation of V_{Sn_2}-H and V_{Ge}-H complexes by introducing H impurities into the divalent cation vacancies. For the first time, we revealed the role of divalent Ge in the formation of *p*-type TCO. By combining the projected densities of states, Bader charge analysis, COOP analysis, and partial charge densities, we revealed that the increase in band gap from α-Sn_3O_4 to α-Sn_2GeO_4 is determined by the weakened interlayer Ge^{2+}-Sn^{2+} interaction and enhanced intralyer Ge^{2+}-O interaction.

Conflicts of interest

There are no conflicts to declare.

Acknowledgements

We acknowledge financial support from the Japan Society for the Promotion of Science (JSPS) through project P14207. This work was partly supported by the Core Research for Evolutional Science and Technology (CREST) program, Materials Research by Information Integration Initiative (MI2I) project of the Japan Science and Technology Agency (JST), Grant-in-Aid for Scientific Research of Japan Society for the Promotion of Science (JSPS) (Grant Numbers JP16K06713 and JP17H03234), and the World Premier International Research Center Initiative on Materials Nanoarchitectonics (MANA), MEXT.

References

1 H. Kawazoe, M. Yasukawa, H. Hyodo, M. Kurita, H. Yanagi, H. Hosono, *P*-type electrical conduction in transparent thin films of $CuAlO_2$, *Nature*, 1997, **389**, 939-942.
2 Y. Ogo, H. Hiramatsu, K. Nomura, H. Yanagi, T. Kamiya, M. Hirano, H. Hosono, *p*-channel thin-film transistor using p-type oxide semiconductor, SnO, *Appl. Phys. Lett.* 2008, **93**, 032113.
3 C. Decroly M. Ghodsi, Sur Lexistence Dun Oxyde Detain De Formule Sn_5O_6, *Comptes Rendus*, 1965, **261**(14), 2659.
4 F. Lawson, Tin Oxide-Sn_3O_4, *Nature* 1967, **215**, 955-956.
5 M. S. Moreno, R. C. Mercader, A. G. Bibiloni, Study of intermediate oxides in SnO thermal decomposition, *J. Phys.: Condens. Matter*, 1992, **4**, 351.
6 M. A. Mäki-Jaskari, T. T. Rantala, Possible structures of nonstoichiometric tin oxide: the composition Sn_2O_3, *Model. Simul. Mater. Sci. Eng.* 2004, **12**, 33-41.
7 A. Seko, A. Togo, F. Oba, I. Tanaka, Structure and Stability of a Homologous Series of Tin Oxides, *Phys. Rev. Lett.*, 2008, **100**, 045702.
8 P. Jackson, K. J. Fisherw, G. D. Willett, Monitoring reagent modification of charged Sn_xO_y nanoclusters using Fourier transform ion cyclotron mass spectrometry, *Phys. Chem. Chem. Phys.*, 2005, **7**, 1687.
9 Y. He, D. Li, J. Chen, Y. Shao, J. Xian, X. Zheng, P. Wang, Sn_3O_4: a novel heterovalent-tin photocatalyst with hierarchical 3D nanostructures under visible light, *RSC Advances*, 2014, **4**, 1266.
10 M. Manikandan, T. Tanabe, P. Li, S. Ueda, G. V. Ramesh, R. Kodiyath, J. Wang, T. Hara, A. Dakshanamoorthy, S. Ishihara, K. Ariga, J. Ye, N. Umezawa, H. Abe, Photocatalytic Water Splitting under Visible Light by Mixed-Valence Sn_3O_4, *ACS Appl. Mater. Interfaces*, 2014, **6**, 3790.
11 J. Wang, N. Umezawa, H. Hosono, Mixed Valence Tin Oxides as Novel van der Waals Materials: Theoretical Predictions and Potential Applications, *Advanced Energy Materials*, 2016, **6**, 1501190.
12 H. Kawazoe, H. Yanagi, K. Ueda, H. Hosono, Transparent Conducting Oxides, *MRS Bulletin*, 2000, **25**(08), 28.
13 H. Mizoguchi, T. Kamiya, S. Matsuishi, H. Hosono, A germanate transparent conductive oxide, *Nature Communications*, 2011, **2**(470), 1.
14 Amit Bhatia, Geoffroy Hautier, Tan Nilgianskul, Anna Miglio, Jingying Sun, Hyung Joon Kim, Kee Hoon Kim, Shuo Chen, Gian-Marco Rignanese, Xavier Gonze, Jin Suntivich, High-Mobility Bismuth-based Transparent *p*-Type Oxide from High-Throughput Material Screening, *Chem. Mater.* **2016**, 28 (1), 30–34.

15 Joel B. Varley, Anna Miglio, Viet-Anh Ha, Michiel J. van Setten, Gian-Marco Rignanese, Geoffroy Hautier, High-Throughput Design of Non-oxide *p*-Type Transparent Conducting Materials: Data Mining, Search Strategy, and Identification of Boron Phosphide, *Chem. Mater.* **2017**, 29 (6), 2568–2573.
16 Viet-Anh Ha, Francesco Ricci, Gian-Marco Rignanese, Geoffroy Hautier, Structural design principles for low hole effective mass *s*-orbital-based p-type oxides, *J. Mater. Chem. C*, **2017**, 5, 5772—5779.
17 A. R. Oganov, C. W. Glass, Crystal structure prediction using ab initio evolutionary techniques: principles and applications, *J. Chem. Phys.*, 2006, **124**, 244704.
18 A. O. Lyakhov, A. R. Oganov, H. T. Stokes, Q. Zhu, New developments in evolutionary structure prediction algorithm USPEX, *Comput. Phys. Commun.*, 2013, **184**, 1172.
19 A. R. Oganov, A. O. Lyakhov, M. Valle, How Evolutionary Crystal Structure Prediction Works-and Why, *Acc. Chem. Res*, 2011, **44**, 227.
20 G. Kresse, J. Furthmuller, Efficiency of ab-initio total energy calculations for metals and semiconductors using a plane-wave basis set, *Comput. Mater. Sci.*, 1996, **6**, 15.
21 J. P. Perdew, M. Ernzerhof, Rationale for mixing exact exchange with density functional approximations, *J. Chem. Phys.*, 1996, **105**, 9982.
22 J. Heyd, G. E. Scuseria, M. J. Ernzerhof, Hybrid functionals based on a screened Coulomb potential, *J. Chem. Phys.*, 2003, **118**, 8207.
23 M. Gajdoš, K. Hummer, G. Kresse, J. Furthmüller, F. Bechstedt, Linear optical properties in the projector-augmented wave methodology, *Phys. Rev. B: Condens. Matter Mater. Phys.*, 2006, **73**(4), 045112.
24 J. B. Varley, A. Schleife, A. Janotti, C. G. Van de Walle, Ambipolar doping in SnO, *Appl. Phys. Lett.*, 2013, **103**, 082118.
25 F. J. Arlinghaus, W. A. Jr. Albers, Electronic energy bands and optical transitions in tetragonal germanium dioxide, *J. Phys. Chem. Solids*, 1971, **32**, 1455-1462.
26 W. H. Strehlow, E. L. Cook, Compilation of Energy Band Gaps in Elemental and Binary Compound Semiconductors and Insulators, *J. Phys. Chem. Ref. Data*, 1973, **2**(1), 163-199.

TOC